CA-17 173

MILITARY TECHNICAL COLLEGE
CAIRO - EGYPT

Numerical and Experimental Determination of Jet Flow Behaviour Through Coaxial Flow Chambers

Tharwat M. Sallam *, Mahmoud H.M. Soliman *,
Osama H. M. Mahmoud**

ABSTRACT

Two-dimensional aerodynamic coaxial flow chamber models are analized and compared with experimental results. Flow patterns, pressure and velocity profiles, jet entrainment and velocity fluctuations are experimentally investigated. Flow patterns are visualized by the tracer method.

Two-dimensional mathematical models of coaxial flow type furnace are examined and aerodynamic characteristics are investigated analytically as well as experimentally. The flow entrainment in the jet mixing zone is investigated. The flow pattern is compared with that of the corresponding plane models.

Numerical calculations using upwind-differencing iterative technique are carried out to determine the flow field behaviour. The computed results are found to be in fair agreement with the experimental measurements.

INTRODUCTION

Two-dimensional models are common for laboratory experimental investigations [1] . The characteristics of the actual coaxial flow chambers are very complicated [2] and [3] . Numerical prediction of flow patterns due to a jet issuing into a bounded space brings about an unsatisfactory results if the boundary conditions and the properties of turbulence, are not appropriate [4] . Experimental observations are, therefore, indispensable for better understanding of the flow fields [5] and [6] .

In the present paper, the characteristics of jet flow through coaxial chamber, which is often used in boiler furnaces and air conditioning ducts are investigated by means of visualization techniques, velocity measurements as well as mathematical models [7] and [8] .

COMPUTATIONS

Numerical solutions of Navier-Stokes equation using upwind-differencing scheme are obtained. The calculations are based on time-dependent approach [9] .

* Lecturer ** Graduate student, Faculty of Engineering, Alexandria University, Egypt.

Momentum equations;

$$\frac{\partial u}{\partial t} + u\frac{\partial u}{\partial x} + v\frac{\partial u}{\partial y} = -\frac{1}{\rho}\frac{\partial p}{\partial x} + \nu\left(\frac{\partial^2 u}{\partial x^2} + \frac{\partial^2 u}{\partial y^2}\right) \quad (1)$$

$$\frac{\partial v}{\partial t} + u\frac{\partial v}{\partial x} + v\frac{\partial v}{\partial y} = -\frac{1}{\rho}\frac{\partial p}{\partial y} + \nu\left(\frac{\partial^2 v}{\partial x^2} + \frac{\partial^2 v}{\partial y^2}\right) \quad (2)$$

continuity equation; $\frac{\partial u}{\partial x} + \frac{\partial v}{\partial y} = 0$ (3)

Vorticity equation;

$$\zeta = \frac{\partial u}{\partial y} - \frac{\partial v}{\partial x} \quad (4)$$

Parapolic transport equation

$$\frac{D\zeta}{Dt} = \nu \nabla^2 \zeta \quad (5)$$

Stream function:

$$u = \frac{\partial \psi}{\partial y} \quad \& \quad v = -\frac{\partial \psi}{\partial x} \quad (6)$$

From eqs. (4) and (6) we get
Poisson elliptic equation;

$$\zeta = \nabla^2 . \psi \quad (7)$$

Eq. (5) is parabolic in time and it needs initial value.

Eq. (7) is elliptic in time and it requires boundary value.

The finite-difference forms for the vorticity and the stream function are;

$$\zeta^n_{i,j} = -\left(\frac{\psi_{i+1,j} - 2\psi_{i,j} + \psi_{i-1,j}}{h^2} + \frac{\psi_{i,j+1} - 2\psi_{i,j} + \psi_{i,j-1}}{h^2}\right) \quad (8)$$

$$\psi_{i,j} = \tfrac{1}{4}\left(\psi_{i+1,j} + \psi_{i-1,j} + \psi_{i,j+1} + \psi_{i,j-1} + h^2 \zeta^n_{i,j}\right) \quad (9)$$

Where; n is the iteration number and h is the node distance.

Boundary condition;

The exit flow value A at point B is correlated with four preceding points. Using Taylor series of expansion to the second derivative. Therefore;

$$A_B = A_{B+4} - 2A_{B+3} + 2A_{B+1} \quad (10)$$

Wall vorticity;

$$\zeta_w = \frac{3}{h^2}\left(\psi_w - \psi_{w+1}\right) - \tfrac{1}{2}\zeta_{w+1} \quad (11)$$

Up stream conditions;

$$\psi = 3y^2 - 2y^3 \quad (12)$$

$$\zeta = -\frac{\partial u}{\partial y} = -6 + 12y \quad (13)$$

Sharp corners;

$$\zeta_c = \psi(i_c, J_{C+1})/(\Delta y)^2 + \psi(i_{c+1}, J_c)/(\Delta x)^2 \quad (14)$$

6

EXPERIMENTAL APPARATUS AND DISCUSSION

The structure of the jet boundaries in the self-preserved region is visualized by the direct injection of condensed milk. A quantitative evaluation of the jet characteristics are recorded by the injection of ignited charcoal particles in the jet downstream. The flow field in the actual chamber is obviously three-dimensional. According to extensive observation with various cold models [10] , however, three-dimensional-flow patterns are similar to that of two-dimensional model test except for the area near the nozzle. Two-dimensional nozzles issuing in a coaxial chamber are adopted in the experimental investigation. Air and water are used as working fluids.

Fig. 1. shows the generation, growth and diffusion of the vortex-street along the axis are very clearly observed. With the increase of velocity, the condensed milk streak line mixes with the surounding water flow with much higher rate. Fig. 2 shows four path line visualization method. In the circulation zone, the velocity is not very high, but it fluctuates due to the generation of different scale vortices in the mixing layer. Fig. 3 and Fig. 4. show a typical flow velocity measurements for eccentric jet and its corresponding turbulence intensity. Fig. 5. shows three different flow patterns at the same Reynolds number, which present clearly a case of jet dynamic instability. Fig. 6 shows two different groups of flow patterns demonstrating a fluctuating flow case and a stable flow condition at a different time of iteration.

RESULTS AND COMPARISON

Typical flow patterns observed in the co-axial cylindrical models for the air flow. When the outer cylinder diameter (D) is large enough compared to the nozzle diameter (d), the main jet reachs the end plate of the channel. Unsymmetrical flow is not observed in the case of axisymmetrical models.

From the comparison between the numerical predictions and the experimented flow patterns, it is found that the numerical method employed yields a good prediction for the flow field.

CONCLUSION

1. The visualized jet structures reveal a clear understanding of the jet behaviour.
2. The jet flow patterns in coaxial chambers are classified according to the jet stability and the type of jet reattachment.
3. The numerical predictions are supported by practical results with actual types.
4. The criterion of jet flow stability is defined experimentally and numerically, within the scope of this research.
5. The predictions by numerical computations represent satisfactory results for the overall flow patterns of the jet coaxial flow models, even in the cases of jet flow instability.

REFERENCES

1. T.M. Sallam, et al., 91 st. Annl. Mt. Ohio State Univ., Apr., (1981), U.S.A.
2. T.M.Sallam, et al., Intr. Symp. on Flow Visualization, Bochum, Sept., (1980), W. Germany.
3. Kawaguti, M., J. Phys., Soc. Japan, 8-6 (1953), P. 747.

4. Son, J.S. and Hanraty, T.J., J. of Fluid Mech., 35-2 (1969), P. 369.

5. K.M. Krall, Ph.D. Thesis, University of Minnesota, (1969).

6. T.M.Sallam, Intr. Symp. on Marine Engng., Tokyo, Oct., (1983), Japan.

7. T.M.Sallam, et al., Proc. of MESJ, Oct., (1980), Japan.

8. Wilkie, D. and Fischer, S.A., Proc. Inst. of Mech. Engng., (1964), P. 461.

9. T.M. Sallam, et al., Intr. Symp. on Flow Visualization, Ann Arbor, Mich., Sept., (1983), U.S.A.

10. T.M. Sallam, Intr. Symp. on Combustion (expected), Mich., Aug., (1984), U.S.A.

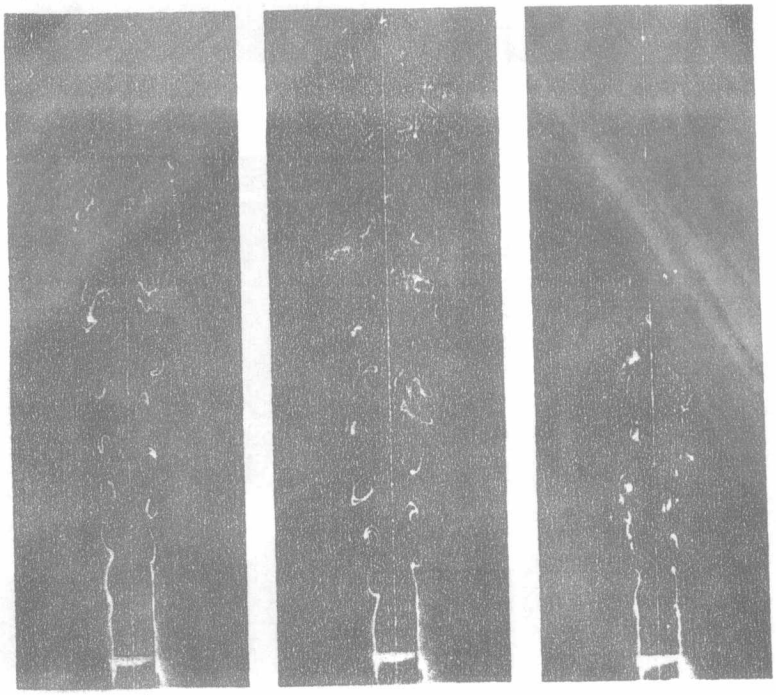

Fig. 1. Jet Structure

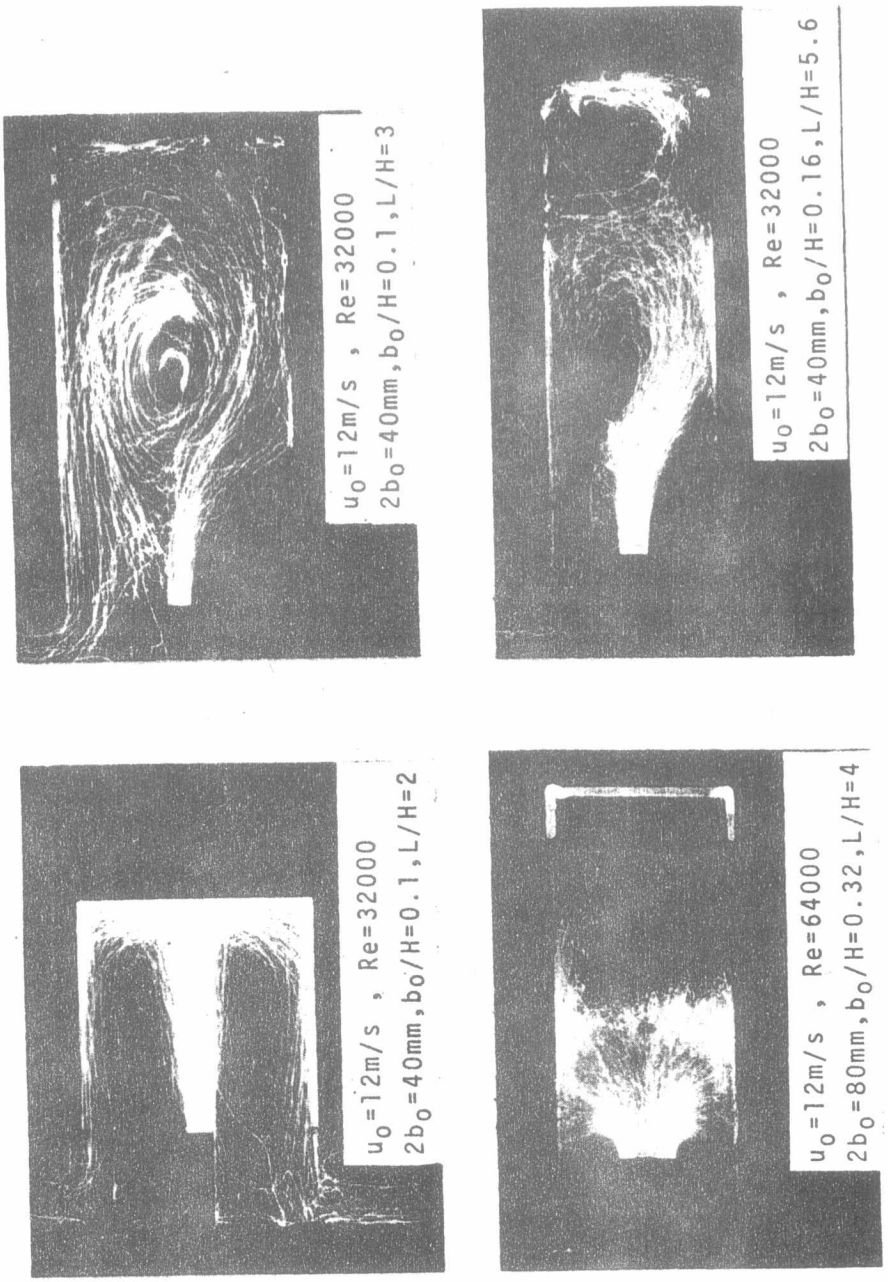

Fig. 2. Flow Patterns for Air Models

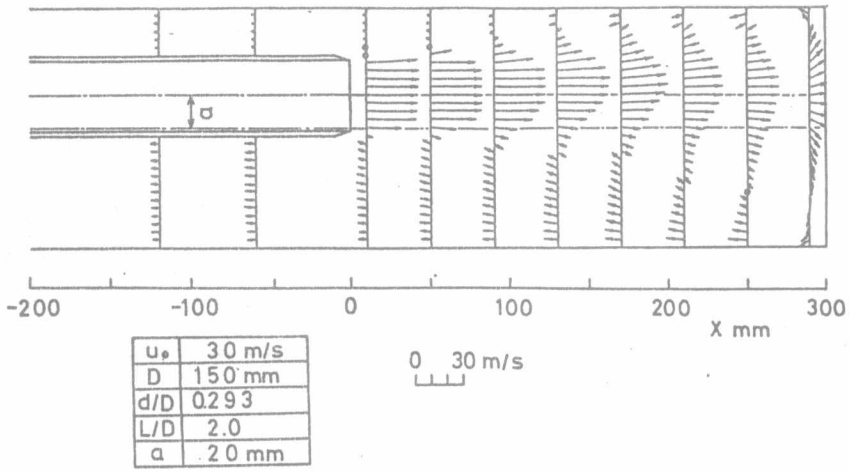

Fig. 3. Velocity Profiles for Eccentric Case

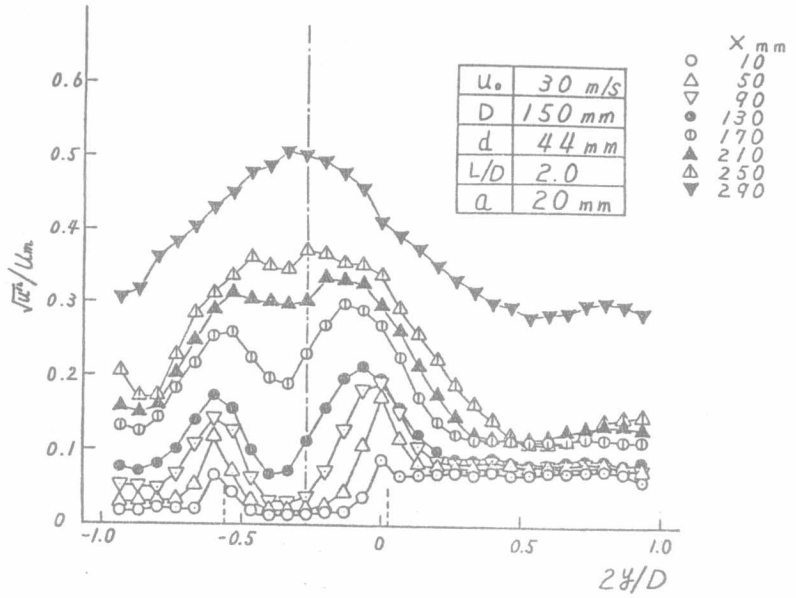

Fig. 4. Turbulence Intensity

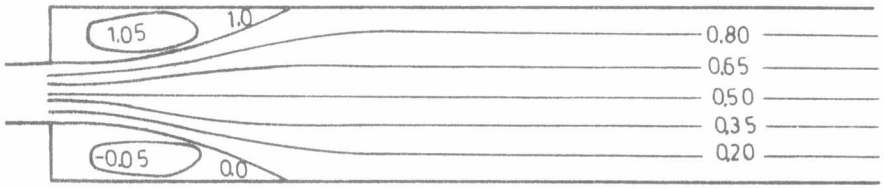

R_e = 130 t = 30

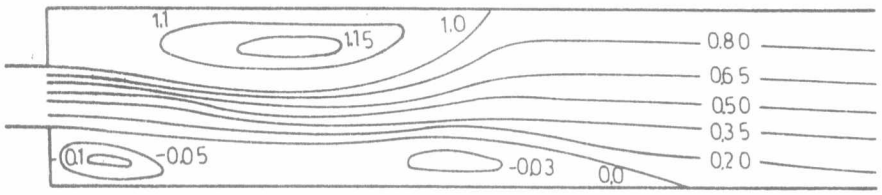

R_e = 130 t = 65

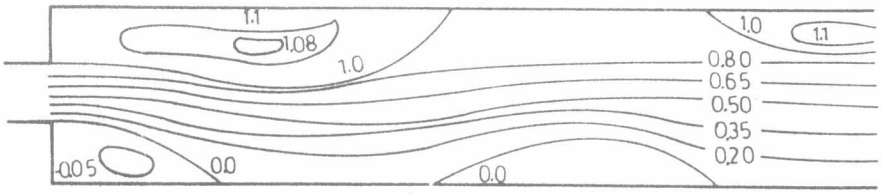

R_e = 130 t = 85

The Flow Pattern Development in a Cylindrical Coaxial Model at a Constant Reynolds Number and Different Time Intervals.

Fig. 5. Flow Pattern Schemes in Cylindrical Coaxial Models.

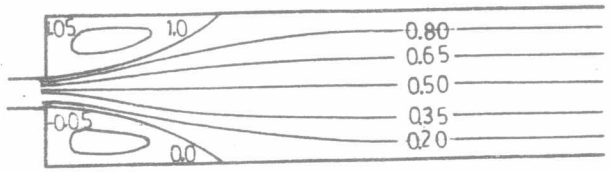

R_e = 40 t = 20

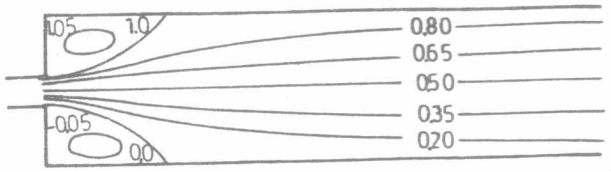

R_e = 80 t = 45

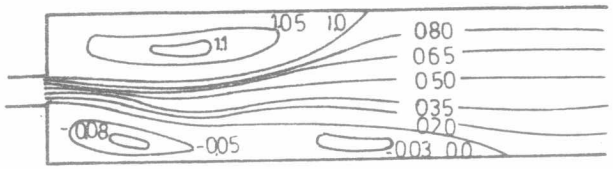

R_e = 120 t = 20

Fluctuating Flow Pattern in a Cylindrical Coaxial Model at Different Reynolds Number

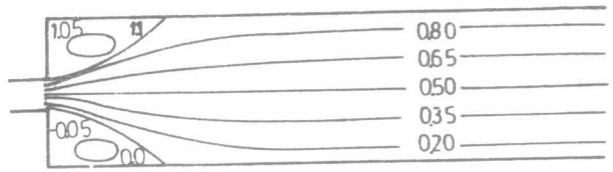

R_e = 80 t = 60

Stable Flow Pattern in a Cylindrical Coaxial Model at Different Time Intervals

Fig. 6. Flow Pattern Schemes in Cylindrical Coaxial Models.